33RD INTERNATIONAL COSMIC RAY CONFERENCE, RIO DE JANEIRO 2013
THE ASTROPARTICLE PHYSICS CONFERENCE

ICRC 2013

Determination of the positron anisotropy with AMS

J. CASAUS[1], ON BEHALF OF THE AMS COLLABORATION[2].

[1] *Centro de Investigaciones Energéticas, Medioambientales y Tecnológicas, CIEMAT, E-28040 Madrid, Spain*
[2] *For the complete list of authors see the AMS Collaboration list in these proceedings.*

Jorge.Casaus@ciemat.es

Abstract: We have studied the cosmic positron anisotropy in the energy range from 16 GeV to 350 GeV on 500,000 positrons and electrons collected during the initial 21 months of operation of AMS on the ISS. The positron to electron ratio is consistent with isotropy at all energies and angular scales throughout this period. A limit on the dipole anisotropy parameter $\delta < 0.030$ at the 95% confidence level for energies above 16 GeV is obtained. The analysis of the positron to proton ratio yields consistent results.

Keywords: AMS, positrons, anisotropy.

1 Introduction

AMS measurement of the positron fraction in primary cosmic rays [1, 2] shows that the positron fraction is steadily increasing from 10 to 250 GeV. This observation is not consistent with the sole secondary production of positrons [3], but requires the inclusion of primary sources, whether from a particle physics or an astrophysical origin [4].

Primary sources of cosmic ray positrons and electrons may induce some degree of anisotropy on the measured positron and electron fluxes [5]. Previous searches have been carried out on the flux of electrons and positrons [6, 7]. In AMS, a systematic search for anisotropies on the positron ratio, that is, the ratio of the positron flux to the electron flux is performed using 500,000 positrons and electrons in the energy range from 16 to 350 GeV collected during the initial 21 months of operations on the ISS, from 19 May 2011 to 10 March 2013.

The positron ratio is computed for different energy ranges and arrival directions in galactic coordinates. The fluctuations of the resulting sky maps are evaluated at several angular scales and upper limits to their amplitude are obtained.

In some models [8], a relative excess of positrons towards the Sun direction is expected. In AMS, this is searched on sky maps constructed in geocentric solar ecliptic coordinates or, likewise, looking for a seasonal excess of the dipole anisotropy in galactic coordinates.

In order to exclude the effect of a supposed anisotropy of the reference electron flux, the analysis has been repeated on the positron to proton ratio.

Finally, the influence of geomagnetic effects is estimated by evaluating the sensitivity to a dipole contribution using the directions obtained after backtracing in the geomagnetic field.

2 The AMS Detector

The Alpha Magnetic Spectrometer (AMS-02) is a general purpose high-energy particle physics detector. It was installed on the International Space Station (ISS) on 19 May 2011 to conduct a unique long duration mission (20 years) of fundamental physics research in space.

The AMS-02 detector [9] consists of nine planes of precision silicon tracker, a transition radiation detector (TRD), four planes of time of flight counters (TOF), a permanent magnet, an array of anticoincidence counters (ACC), surrounding the inner tracker, a ring imaging Čerenkov detector (RICH), and an electromagnetic calorimeter (ECAL).

3 Data Selection

Electron and positron selection for this analysis follows that described in [1] and [2].

The reduction of the proton background in the identification of the positron and electron samples is achieved by means of the TRD, the ECAL and the tracker. Events are selected by requiring a track in the TRD and in the tracker, a cluster of hits in the ECAL, and a measured velocity $\beta \sim 1$ in the TOF consistent with a downward-going Z = 1 particle. Protons are rejected by requiring a good energy-momentum matching and explicit cuts on the ECAL and TRD estimators.

The overall selection efficiency for positrons and electrons is estimated to be above 80% in the acceptance of the ECAL. The remaining sample contains 35,000 primary positrons, 460,000 electrons and a negligible amount of protons.

The selected events are grouped into 5 cumulative energy ranges from 16 to 350 GeV according to their measured energy in the ECAL. The minimum energies are 16, 25, 40, 65 and 100 GeV, respectively.

4 Anisotropy on e^+/e^-

The arrival directions of electrons and positrons are used to build sky maps in galactic coordinates, (b,l), containing the number of observed positrons and electrons. The maps corresponding to electrons and positrons in the energy range from 16 to 350 GeV are displayed in Fig. 1. The spread of the number of events collected on different directions is a consequence of the non uniform sky coverage of the AMS exposure.

Different approaches have been followed to define the binning on the sky maps. First, same area rectangular bins are defined on the $(\sin(b),l)$ plane and regions with low exposure are excluded from the analysis. Second, rectangular bins mapping similar exposure, that is, containing same

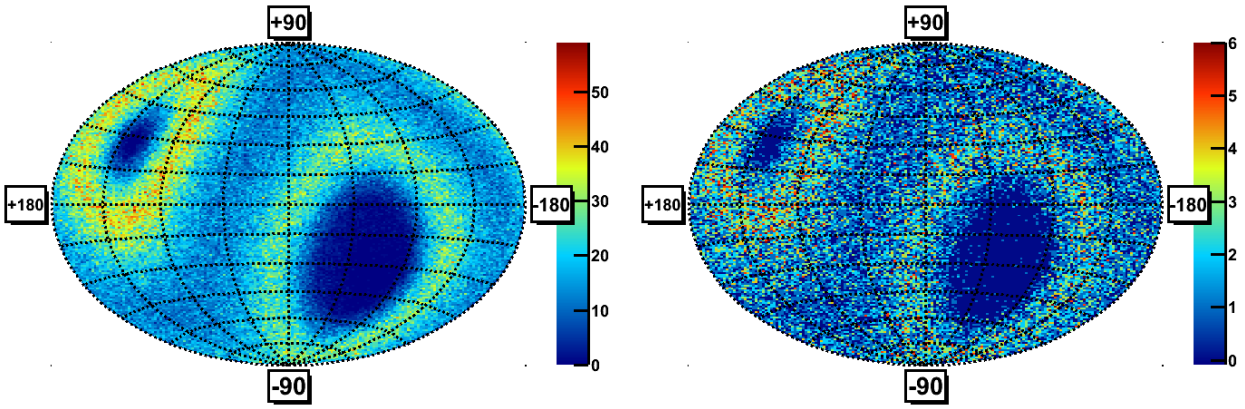

Fig. 1: Sky maps showing the arrival directions of selected 16–350 GeV electrons (left) and positrons (right) in galactic coordinates using a Hammer-Aitoff projection. The color code reflects the number of events per bin.

number of electrons, are defined. The comparison of the results obtained on different binning is used to estimate the stability of the analysis.

For a given energy range, the positron to electron ratio is computed on each galactic coordinate bin. The consistency of the set of bin-to-bin ratios to a common value is estimated using a χ^2 test. A good agreement is found for all energy ranges. Moreover, no structure is observed on the projections along galactic latitude or longitude.

A general description of the relative fluctuations on the observed positron ratio is obtained by means of a spherical harmonic expansion

$$\frac{r_e(b,l)-\langle r_e\rangle}{\langle r_e\rangle} = \sum_{\ell=0}^{\infty}\sum_{m=-\ell}^{\ell} a_{\ell m}\, Y_{\ell m}(\pi/2-b,l),$$

where $r_e(b,l)$ denotes the positron ratio at (b,l), $\langle r_e\rangle$ is the average ratio over the sky map, $Y_{\ell m}$ are the real spherical harmonic functions, and a_{lm} are their corresponding amplitudes.

The amplitudes of spherical harmonic contributions at fixed angular scale, ℓ, are fit to the data for dipole ($\ell = 1$), quadrupole ($\ell = 2$) and octopole ($\ell = 3$) contributions with a χ^2 minimization. No significant a_{lm} is found at any angular scale ($\ell = 1,2,3$) and energy range. As an example, in Fig. 2 the results corresponding to a dipole contribution perpendicular to the galactic plane, a_{10}, are displayed together with the 1, 2 and 3σ contours as a function of the minimum energy. Similar sensitivity is obtained on the amplitudes of the other spherical harmonic contributions.

The intensity of the fluctuations on the studied angular scales is quantified with the coefficients of the angular power spectrum defined as

$$C_\ell = \frac{1}{2\ell+1}\sum_{m=-\ell}^{\ell} a_{\ell m}^2.$$

The values of the coefficients C_1, C_2 and C_3 obtained from the fits are consistent with the expectations from pure statistical fluctuations on all energy ranges. The results for the dipole coefficient C_1 are shown in Fig. 3 along with expected level for random noise and its 68% CL band.

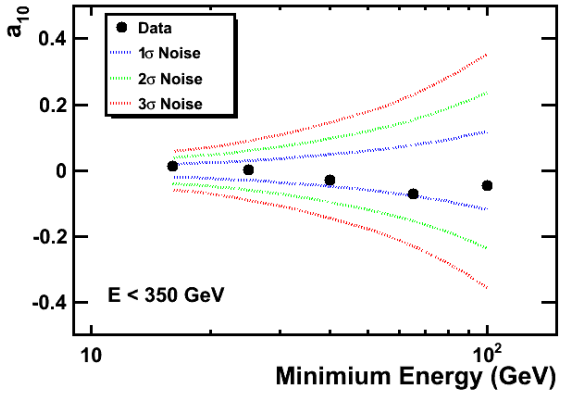

Fig. 2: Amplitudes a_{10} obtained from fits of a dipole contribution to the data on different energy ranges. The dashed lines correspond to the 1, 2 and 3σ contours.

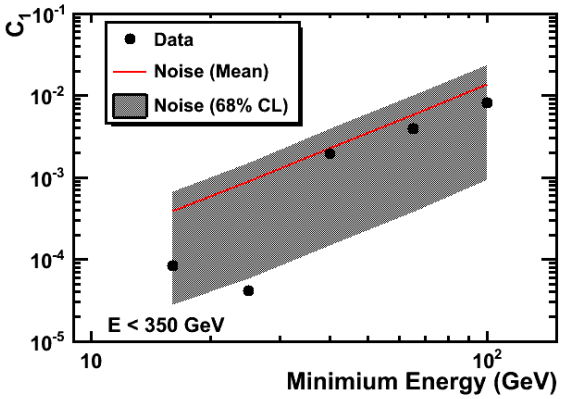

Fig. 3: Results for the dipole coefficient C_1 obtained from the fits to the data on different energy ranges. The expected level for random noise together with its 68% CL band is also displayed.

4.1 Dipole Anisotropy

The anisotropy induced by primary sources is expected to follow a dipole pattern with the maximum pointing towards the source and the minimum to the opposite direction. It is then customary to define the dipole anisotropy parameter, δ, as the relative difference between maximum and minimum amplitudes. Therefore, δ can be derived from the coefficient C_1 with the expression $\delta = 3\sqrt{C_1/4\pi}$.

Since the coefficients of the multipole expansion are consistent with the expectations from isotropy, limits on the coefficients of the angular power spectrum, C_l, can be obtained for all energy ranges. In particular, limits on the dipole anisotropy parameter δ are derived for any axis in galactic coordinates. The upper limits at the 95% confidence level for the 5 cumulative energy ranges are shown in Fig 4. The limit obtained for the energy range from 16 to 350 GeV is $\delta < 0.030$.

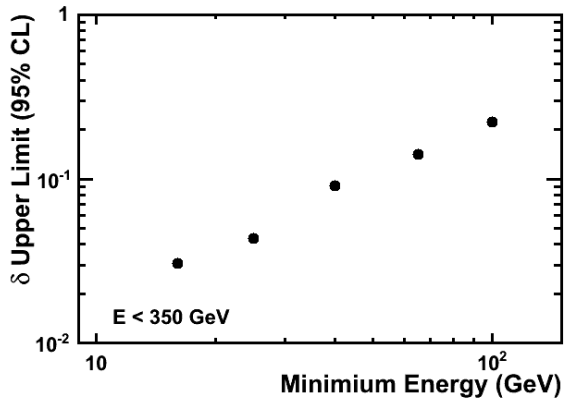

Fig. 4: AMS upper limits on the dipole anisotropy parameter δ at the 95% confidence level on different energy ranges.

This value corresponds to the fit of the sky map with 20x20 bins where only bins with at least 50 electrons are considered. The fraction of masked channels is 3.5% and the χ^2 of the fit to a dipole contribution is 390.3 for 382 degrees of freedom.

The stability of the results is verified by repeating the analysis on sky maps constructed with different binning. First, the number of bins in the regular binning is changed in a wide range, namely from 4x4 bins to 40x40 bins. Second, the same analysis is carried out using adaptive bins mapping the AMS exposure. In all cases, negligible differences are found.

The influence of the masked bins in the sky maps is also explored by changing the requirement on the minimum number of electrons from 25 to 200 events per bin, which modifies the number of bins participating in the fit in about 10%. Again, no significant difference is found.

4.2 Seasonal Excess

Dark matter annihilation in the Sun vicinity could generate a relative positron excess towards the Sun direction. When integrated over a complete year, the dominant dipole contribution would effectively cancel on the sky maps computed in galactic coordinates. However, seasonal effects may be observed.

The data is divided into 8 seasons covering the whole data taking period and the analysis is repeated on the individual samples. No significant deviation from isotropy is found. As an example, in Fig. 5 the values obtained for the dipole coefficient C_1 on the different samples for the energy range 16 to 350 GeV are displayed relative to the expected noise level. Data is consistent with the expectations from pure statistical fluctuations.

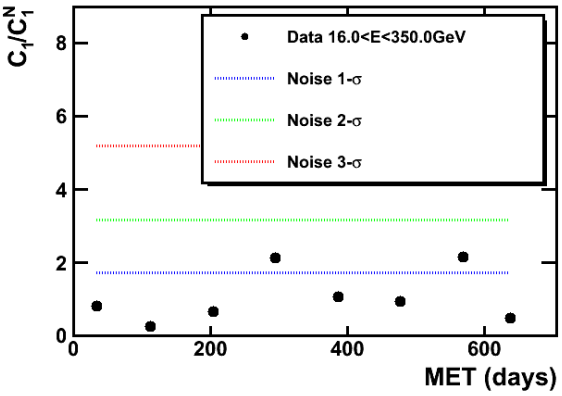

Fig. 5: Dipole coefficients C_1 obtained from the fit to the data in the energy range 16 to 350 GeV corresponding to the 8 seasons covering the whole data taking period. The values are displayed relative to the expected noise level for random fluctuations. The dashed lines correspond to the 1, 2 and 3σ upper contours.

The effect of an excess towards the Sun direction is enhanced on the appropriate reference system. A complementary analysis is performed using sky maps built in geocentric solar ecliptic coordinates, where the Earth-Sun axis defines its primary direction and its equatorial plane lies on the ecliptic. No significant deviation from isotropy is found and similar limits on a dipole anisotropy as those obtained in Sec. 4.1 are derived.

5 Anisotropy on e^+/p

The use of protons as the reference for the measurement of the positron anisotropy has the advantage of removing the effect of a possible anisotropy in the electron flux. In addition, the influence of geomagnetic effects can be estimated by evaluating the sensitivity to a dipole contribution using the directions obtained after backtracing in the geomagnetic field, thus investigating such an effect at the entrance of magnetosphere. The analysis has thus been repeated on the positron to proton ratio.

A pure proton sample covering the same angular acceptance as the positron and electron samples is achieved by reversing the cuts on the ECAL and TRD estimators. The selected protons are classified into the energy ranges defined in Sec. 3 according to their measured rigidity.

The sensitivity to a dipole anisotropy using the positron to proton ratio is compatible with that obtained on the positron to electron analysis within 5% and the results are consistent with those presented in Sec. 4.

The analysis is repeated on the maps built using the asymptotic directions obtained after backtracing their trajectories in the geomagnetic field to the border of the Earth's

magnetosphere [1] [10, 11]. The geomagnetic field model includes the IGRF-11 [12] description of the internal field and Tsyganenko 1996 and 2005 models [13, 14] for the external field.

Similar sensitivity to a dipole anisotropy is found after backtracing (see Fig. 6). For the high energy ranges no deviation is found. At lower energies the sensitivities inside and outside the magnetosphere differ by about 10-20%. This is due to the effect of the geomagnetic field which makes more uniform particle distributions inside magnetosphere, while, after backtracing, the direction of low energy events is focused towards the equatorial plane. In Fig. 7 the amplitude of a_{11} for e^+/p is shown for data observed at ISS orbit and at the border of the magnetosphere. Using the real spherical harmonics functions, the physical dipole component along the radial galactic direction can be written as $\rho_{\rm FB} = \sqrt{3/4\pi}\, a_{11}$.

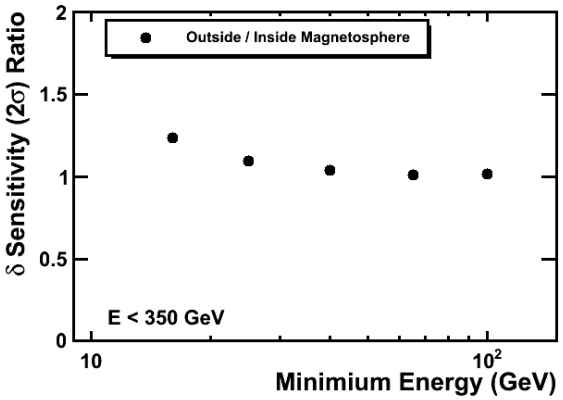

Fig. 6: Ratio of the 2σ sensitivity to a dipole contribution from the analyses outside and inside the magnetosphere.

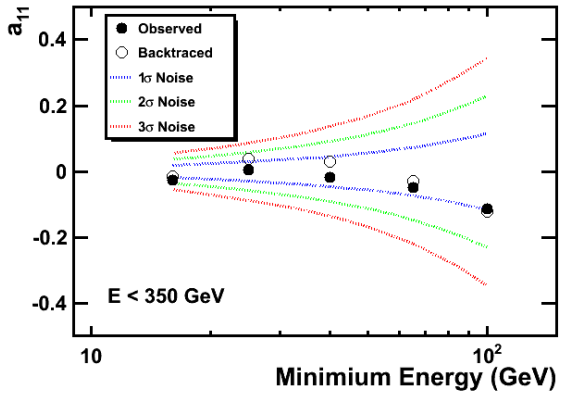

Fig. 7: Comparison of the amplitudes a_{11} obtained from fits of a dipole contribution to the data on different energy ranges using the observed and backtraced directions. See text for its relation with the $\rho_{\rm FB}$ dipole component. The dashed lines correspond to the 1, 2 and 3σ contours.

6 Conclusions

A systematic search for anisotropies on the cosmic ray positrons is performed on a sample of 35,000 positrons selected in the energy range from 16 to 350 GeV.

No anisotropy is found on the positron to electron ratio at any angular scale on the sky maps built on the arrival directions in galactic coordinates. The upper limits are set on the dipole anisotropy parameter δ. The 95% confidence level limit obtained for the energy range from 16 to 350 GeV is $\delta < 0.030$.

No indication of seasonal excess is observed on the estimated positron anisotropy in galactic coordinates and no enhancement is detected on the maps built in solar ecliptic coordinates as expected from dark matter annihilation in the Sun vicinity.

Consistent results are obtained on the positron to proton ratio and equivalent limits are computed after backtracing particle trajectories in the geomagnetic field to the border of the Earth's magnetosphere.

Acknowledgments: This work has been supported by persons and institutions acknowledged in [1], as well as by the Italian Space Agency under contracts ASI-INFN I/002/13/0 and ASDC/011/11/1.

References

[1] M. Aguilar et al. (AMS Collaboration), Phys. Rev. Lett. 110, 141102 (2013).
[2] A. Kounine et al. (AMS Collaboration), this conference.
[3] T. Delahaye, R. Lineros, F. Donato, N. Fornengo, J. Lavalle, P. Salati, and R. Taillet, Astron. Astrophys. 501, 821 (2009); I. Moskalenko and A. Strong, Astrophys. J. 493, 694 (1998).
[4] P. D. Serpico, Astropart. Phys. 39-40, 2 (2012); N. Arkani-Hamed, D. P. Finkbeiner, T. R. Slatyer and N. Weiner, Phys. Rev. D, 79, 015014 (2009); D. Hooper, P. Blasi and P. D. Serpico, Journal of Cosmology and Astropart. Phys. 01 (2009) 025.
[5] I. Büsching, O.C. de Jager, M.S. Potgieter and C. Venter, Astrophys. J. 678 (2008) L39; I. Cernuda, Astropart. Phys. 34 (2010) 59.
[6] M. Ackermann et al. (The Fermi LAT Collaboration), Phys. Rev. D 82, 092003 (2010).
[7] D Campana et al. (PAMELA Collaboration), 2013 J. Phys.: Conf. Ser. 409 012055.
[8] P. Schuster, N. Toro, N. Weiner and I. Yavin, Phys.Rev.D82:115012,2010
[9] A. Kounine, Int. J. Mod. Phys. E 21, 1230005 (2012); Samuel C. C. Ting, in Proceedings of the 4th International Conference on Particle and Fundamental Physics in Space, Geneva (to be published); S.-C. Lee, in Proceedings of the Twentieth International Conference on Supersymmetry and Unification of Fundamental Interactions (SUSY 2012), Beijing, China (to be published); M. Aguilar, in Proceedings of the XL International Meeting on Fundamental Physics, Centro de Ciencias de Benasque Pedro Pascual (to be published); S. Schael, in Proceedings of the Tenth Symposium on Sources and Detection of Dark Matter and Dark Energy in the Universe, Los Angeles (to be published); B. Bertucci, Proc. Sci., EPS-HEP (2011) 67; M. Incagli, AIP Conf. Proc. 1223, 43 (2009); R. Battiston, Nucl. Instrum. Methods Phys. Res., Sect. A 588, 227 (2008).
[10] P. Bobik et al., this conference.
[11] M. Boschini et al., this conference.
[12] C. C. Finlay et al. Geophysical Journal International (2010) 183 (3) 1216.
[13] N. A. Tsyganenko, Journal of Geophysical Research v. 100 (1995) A4 5599.
[14] N. A. Tsyganenko, Journal of Geophysical Research v. 110 (2005) A0 3208.

1. http://www.geomagsphere.org/